

## Roasting and leaching behaviors of vanadium and chromium in calcification roasting–acid leaching of high-chromium vanadium slag

Jing Wen<sup>1)</sup>, Tao Jiang<sup>1,2)</sup>, Mi Zhou<sup>1,2)</sup>, Hui-yang Gao<sup>1)</sup>, Jia-yi Liu<sup>1)</sup>, and Xiang-xin Xue<sup>1,2)</sup>

1) School of Metallurgy, Northeastern University, Shenyang 110819, China

2) Liaoning Key Laboratory for Recycling Science of Metallurgical Resources, Shenyang 110819, China

(Received: 13 September 2017; revised: 8 November 2017; accepted: 23 November 2017)

**Abstract:** Calcification roasting–acid leaching of high-chromium vanadium slag (HCVS) was conducted to elucidate the roasting and leaching behaviors of vanadium and chromium. The effects of the purity of CaO, molar ratio between CaO and  $V_2O_5$  ( $n(\text{CaO})/n(\text{V}_2\text{O}_5)$ ), roasting temperature, holding time, and the heating rate used in the oxidation–calcification processes were investigated. The roasting process and mechanism were analyzed by X-ray diffraction (XRD), scanning electron microscopy (SEM), and thermogravimetry–differential scanning calorimetry (TG–DSC). The results show that most of vanadium reacted with CaO to generate calcium vanadates and transferred into the leaching liquid, whereas almost all of the chromium remained in the leaching residue in the form of  $(\text{Fe}_{0.6}\text{Cr}_{0.4})_2\text{O}_3$ . Variation trends of the vanadium and chromium leaching ratios were always opposite because of the competitive reactions of oxidation and calcification between vanadium and chromium with CaO. Moreover, CaO was more likely to combine with vanadium, as further confirmed by thermodynamic analysis. When the HCVS with CaO added in an  $n(\text{CaO})/n(\text{V}_2\text{O}_5)$  ratio of 0.5 was roasted in an air atmosphere at a heating rate of  $10^\circ\text{C}/\text{min}$  from room temperature to  $950^\circ\text{C}$  and maintained at this temperature for 60 min, the leaching ratios of vanadium and chromium reached 91.14% and 0.49%, respectively; thus, efficient extraction of vanadium from HCVS was achieved and the leaching residue could be used as a new raw material for the extraction of chromium. Furthermore, the oxidation and calcification reactions of the spinel phases occurred at 592 and  $630^\circ\text{C}$  for  $n(\text{CaO})/n(\text{V}_2\text{O}_5)$  ratios of 0.5 and 5, respectively.

**Keywords:** high-chromium vanadium slag; calcification roasting; roasting behaviors; leaching behaviors; vanadium extraction

### 1. Introduction

Vanadium, chromium, and their compounds are significant strategic resources that play important roles in the development of modern technology and industry [1]. In China, the main feedstock for vanadium recovery is vanadium–titanium-bearing magnetite [2], which is a complex ore that contains iron, vanadium, titanium, and other valuable elements such as chromium. During the smelting process using vanadium–titanium-bearing magnetite, vanadium and chromium with similar chemical characteristics are reduced into molten pig iron by coke in a blast furnace and then oxidized and enriched into vanadium slag in a vanadium-extracting converter [3]. The vanadium slag currently used for large-scale industrial production and systematic laboratory studies has a low chromium content [4]. Vanadium slag with high-chromium content is gradually attracting

more attention because of its massive reserves and potential threat to the environment [5]. Zhang *et al.* [6] investigated and compared the oxidation behavior of vanadium in high-chromium vanadium slag (HCVS) during blank roasting with conventional roasting and microwave-assisted roasting. Li *et al.* [7] treated HCVS using sodium roasting–water leaching and found that almost all of the chromium was transferred to the leaching liquid with vanadium. Liu *et al.* [3] reported a new method to extract vanadium and chromium simultaneously and efficiently from vanadium slag containing chromium using a molten  $\text{NaOH}$ – $\text{NaNO}_3$  binary system. In addition, on the basis of the nucleation and growth kinetics of spinel crystals in vanadium slag, Li *et al.* [8] proposed the asynchronous extraction of vanadium and chromium from vanadium slag by stepwise sodium roasting–water leaching.

Roasting plays a critical role throughout the process of

Corresponding author: Tao Jiang E-mail: [jiangt@smm.neu.edu.cn](mailto:jiangt@smm.neu.edu.cn)

© University of Science and Technology Beijing and Springer-Verlag GmbH Germany, part of Springer Nature 2018

vanadium extraction. At present, sodium salt roasting is the most commonly used technology for the pretreatment of vanadium slag [9], through which vanadium(III) is oxidized to sodium vanadate(V). Nevertheless, sodium salt roasting generates a considerable amount of harmful gases such as  $\text{Cl}_2$  and  $\text{SO}_2$  via the decomposition of sodium salts such as  $\text{NaCl}$  and  $\text{Na}_2\text{SO}_4$ . Furthermore, sodium salts with low melting points tend to agglomerate during roasting, hindering the further oxidation of vanadium and decreasing its extraction [10]. Regarding the roasting and leaching behaviors of chromium during sodium salt roasting, several studies have found that chromium(III) can be oxidized to soluble sodium chromate(VI) and converted into leaching liquor along with sodium vanadium [11]. The toxic solution containing chromium cannot be appropriately disposed of after vanadium extraction and is a potential threat to humans, animals, and the environment. In addition, complete separation of vanadium and chromium is difficult because of their similar chemical properties in solution. Several articles have reported separation methods based on reduction–precipitation [12], solvent extraction [13], and ion exchange [14], among other methods, which also introduce problems such as high cost, long flowsheets, and complex processing.

Calcification roasting, proposed by the Russia Fula factory in the 1970s, is a more environmentally friendly alternative to sodium salt roasting [15]. During calcification roasting, lime or limestone is added to the vanadium slag to transform vanadium-bearing spinels into water-insoluble calcium vanadates such as  $\text{CaV}_2\text{O}_6$ ,  $\text{Ca}_2\text{V}_2\text{O}_7$ , and  $\text{Ca}_3\text{V}_2\text{O}_8$  [16]. This process avoids the emission of harmful gases and a health crisis from toxic and carcinogenic soluble vana-

dium(V). Recently, numerous researchers have investigated the effects of roasting parameters, including the  $m(\text{CaO})/m(\text{V}_2\text{O}_5)$  ratio, roasting temperature, and the holding time on the vanadium extraction during the calcification roasting process, along with the mechanism of calcification roasting [17]. However, little attention has been devoted to the extraction behavior of chromium during calcification roasting with HCVS. Furthermore, with the discovery of large-scale high-chromium vanadium–titanium-bearing magnetite, such as Hongge ore in Panzhihua, China, research into chromium extraction has become urgent. It is important to discuss whether chromium transfers into the leaching liquid with vanadium or remains in the leaching residue, which is critical for vanadium and chromium separation in the subsequent stage and is an important topic.

In this study, the roasting and leaching behaviors of vanadium and chromium are discussed. Roasting conditions, including the purity of  $\text{CaO}$ , the  $n(\text{CaO})/n(\text{V}_2\text{O}_5)$  ratio, roasting temperature, holding time, and the heating rate, are optimized. Further, an oxidation and calcification process of spinel phases in HCVS is proposed.

## 2. Experimental

### 2.1. Materials

The raw material, HCVS, was obtained from Chengde Jianlong Iron and Steel Co., Ltd., China. The main chemical components and the X-ray diffraction (XRD) pattern of the HCVS are presented in Table 1 and Fig. 1, respectively, and the backscatter image and energy-dispersive spectroscopy (EDS) element mapping images of HCVS are displayed in

Table 1. Chemical composition of HCVS

wt%

TFe	FeO	MFe	$\text{V}_2\text{O}_5$	$\text{Cr}_2\text{O}_3$	$\text{TiO}_2$	$\text{SiO}_2$	$\text{Al}_2\text{O}_3$	CaO	MnO	MgO	$\text{P}_2\text{O}_5$
33.82	23.50	4.52	13.72	9.19	10.45	14.62	1.30	1.67	6.73	1.17	0.12

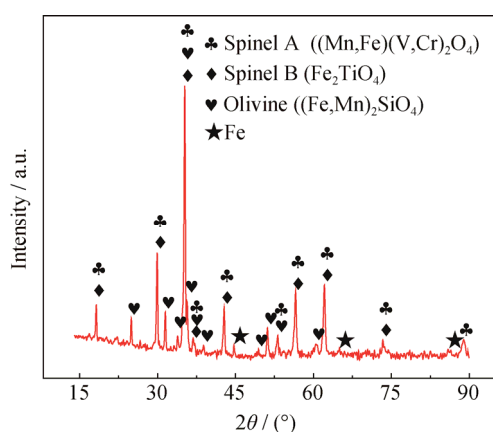


Fig. 1. XRD pattern of the HCVS used in this study.

Fig. 2. The results show that the chromium content in this slag is high. From the perspective of crystallization of vanadium slag during its converter-extraction process [18–19], vanadium, chromium, and titanium all exist in the form of spinels, and the crystallization ability of these three spinel phases follows the order  $\text{FeCr}_2\text{O}_4 > \text{FeV}_2\text{O}_4 > \text{Fe}_2\text{TiO}_4$ . Both vanadium and chromium exist mainly in the form of the spinel phase  $(\text{Mn,Fe})(\text{V,Cr})_2\text{O}_4$ , which is further confirmed by scanning electron microscopy (SEM) with EDS element mapping of HCVS. Titanium exists in the form of spinel  $\text{Fe}_2\text{TiO}_4$ . The spinel phase is dispersed in the olivine phase  $(\text{Fe,Mn})_2\text{SiO}_4$ , in which a large amount of silicon is concentrated. Iron is present in all of the regions, and a

small amount of iron exists in HCVS in the form of free metallic iron. All of the aforementioned characteristics of

the HCVS are consistent with those of other vanadium slags.

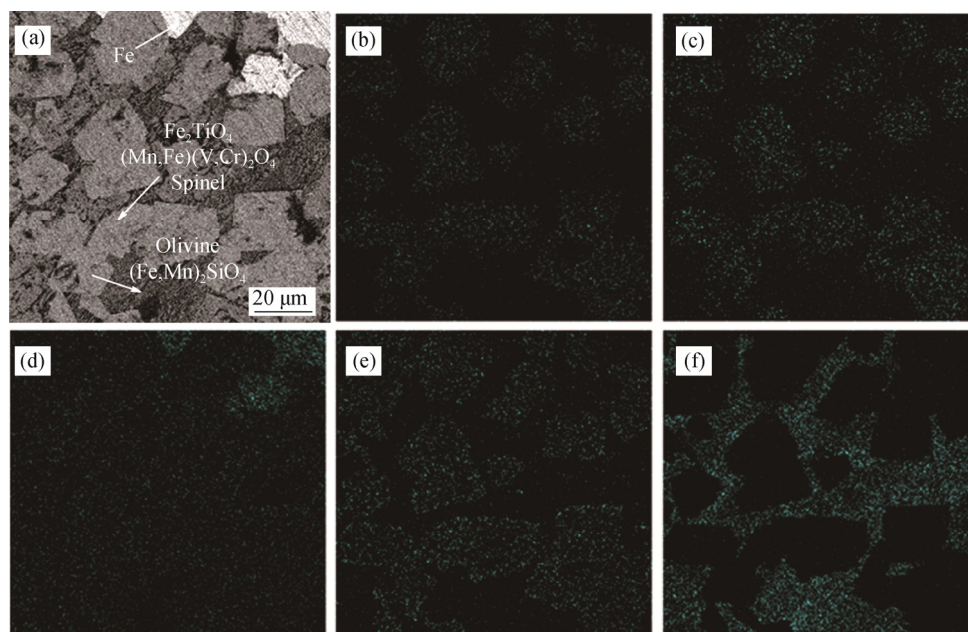


Fig. 2. Backscattered electron image (a) and EDS element mapping images of Fe (b), V (c), Cr (d), Ti (e), and Si (f) in the HCVS used in this study.

In addition, the CaO additive was dried in an oven at 105°C for 24 h prior to use, and its XRD pattern is shown in Fig. 3. The result shows that a small amount of  $\text{Ca(OH)}_2$  is present because CaO tends to react with water molecules in the air to form  $\text{Ca(OH)}_2$ . This situation is inevitable and cannot be neglected, and it becomes more obvious with time. Hence, it is critical to investigate the effects of the purity of CaO on vanadium and chromium extraction.

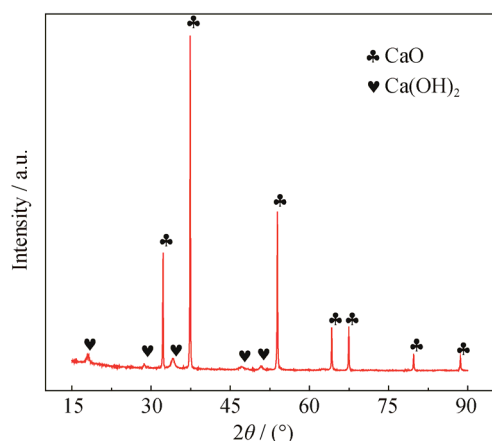


Fig. 3. XRD pattern of CaO.

All aqueous solutions were prepared with distilled water. Other chemical reagents, including  $\text{H}_2\text{SO}_4$ ,  $(\text{NH}_4)_2\text{Fe}(\text{SO}_4)_2 \cdot 6\text{H}_2\text{O}$ ,  $\text{C}_{13}\text{H}_{11}\text{NO}_2$ ,  $\text{H}_2\text{NCONH}_2$ ,  $\text{NaNO}_2$ , and  $\text{KMnO}_4$ , were all analytical-grade reagents.

## 2.2. Experimental procedures

### 2.2.1. Calcification roasting

In the calcification roasting process, HCVS powder ( $< 74 \mu\text{m}$ , 10 g) was mixed with CaO (0–2.111 g) in  $n(\text{CaO})/n(\text{V}_2\text{O}_5)$  ratios from 0 to 5. The mixtures were loaded into porcelain crucibles separately and heated in a temperature-controlled muffle furnace at 600–950°C for 0–3 h at a heating rate of 2–30°C/min. During the roasting process, the door of the muffle furnace was not completely closed to maintain a constant oxidizing atmosphere. After roasting, the roasted samples were cooled slowly in the furnace and then ground into powders.

### 2.2.2. Acid leaching

Leaching experiments were performed in conical flasks placed in a commercial magnetic stirring water bath pot (type DF-101, Gongyi Electric Equipment Corp., China). A leaching medium with higher acidity was used in the experiments to ensure complete dissolution of the vanadate. The roasted samples were leached under appropriate leaching conditions based on our experiments and other research results. Leaching experiments were conducted using sulfuric acid at a specific concentration of 20vol%, solid-to-liquid mass ratio ( $m_{\text{roasted samples}}/m_{\text{H}_2\text{SO}_4}$ ) of 1:5, a leaching temperature of 70°C, a leaching time of 1 h, and a stirring speed of 200 r/min. After the leaching process, a filtration step was

carried out to collect the leaching liquor and leaching residue separately. The leaching liquor was repeatedly washed with distilled water at 70°C until the washing fluids were pH-neutral; the leaching liquor was subsequently diluted to 1000 mL.

The leaching ratio (LR) of vanadium or chromium was calculated using the following equation:

$$LR = \frac{m_L}{m_0} \times 100\% \quad (1)$$

where  $m_0$  is the mass of vanadium or chromium in HCVS after roasting, and  $m_L$  is the mass of vanadium or chromium in the leaching liquor after leaching. The filtrate was analyzed using the ferrous ammonium sulfate titration method to determine the amount of vanadium, and the concentration of total chromium was analyzed using an atomic absorption spectrophotometer (TAS-990, Beijing Purkinje General Instrument Co. Ltd.) [20].

### 2.2.3. Characterization

The chemical compositions of the HCVS samples were determined by inductively coupled plasma–atomic emission spectroscopy (ICP–AES, PerkinElmer Optima-4300DV) (except for FeO and MFe, which were analyzed by chemical analysis). The phase compositions of the solid samples were identified by XRD analysis (X'PERT PRO MPD/PW3040, PANalytical B.V. Corp., The Netherlands) using Cu K $\alpha$  radiation for 10 min in a  $2\theta$  range of 15° to 90°. The microscopic observation and analysis of the element distribution in the samples were conducted by SEM on a scanning electron microscope (TESCAN VEGA III) equipped with an EDS spectrometer (INCA Energy 350). Thermogravimetry (TG) and differential scanning calorimetry (DSC) were carried out with a TA Instruments SDT-Q600 simultaneous DSC-TGA; the analyses were carried out at a heating rate of 10°C/min from room temperature to 1000°C.

## 3. Results and discussion

### 3.1. Thermodynamic analysis of the roasting process

The main chemical reactions of vanadium and chromium during calcification roasting with HCVS are summarized in Table 2, and the relationships between temperature and standard Gibbs free energy changes ( $\Delta_r G^\ominus$ ), as calculated using the HSC Chemistry version 6.0 software, are shown in Fig. 4. The  $\Delta_r G^\ominus$  of these reactions (except for the formation of calcium chromate) are negative over the temperature range from 200 to 1000°C, indicating that the oxidation of spinels and the formation of vanadates are thermodynamically feasible. Further, the  $\Delta_r G^\ominus$  of reaction (2) is more negative than that of reaction (3), implying that the V-spinel

is more easily decomposed than the Cr-spinel. The  $\Delta_r G^\ominus$  values for reactions (5) to (8) show that calcium vanadate is more stable than calcium chromate and that CaO may be more likely to combine with vanadium. In addition, Cr<sup>3+</sup> tends to be oxidized to form CaCrO<sub>4</sub>, particularly at lower temperatures (200–800°C). With increasing temperature, other chromates such as Ca<sub>3</sub>(CrO<sub>4</sub>)<sub>2</sub> may form instead of CaCrO<sub>4</sub> [21].

**Table 2. Main chemical reactions during calcification roasting with HCVS and CaO**

Reaction	No.
$4\text{FeV}_2\text{O}_4 + \text{O}_2(\text{g}) \rightleftharpoons 2\text{Fe}_2\text{O}_3 + 4\text{V}_2\text{O}_3$	(2)
$4\text{FeCr}_2\text{O}_4 + \text{O}_2(\text{g}) \rightleftharpoons 2\text{Fe}_2\text{O}_3 + 4\text{Cr}_2\text{O}_3$	(3)
$\text{V}_2\text{O}_3 + \text{O}_2(\text{g}) \rightleftharpoons \text{V}_2\text{O}_5$	(4)
$\text{V}_2\text{O}_5 + \text{CaO} \rightleftharpoons \text{CaV}_2\text{O}_6$	(5)
$\text{V}_2\text{O}_5 + 2\text{CaO} \rightleftharpoons \text{Ca}_2\text{V}_2\text{O}_7$	(6)
$\text{V}_2\text{O}_5 + 3\text{CaO} \rightleftharpoons \text{Ca}_3\text{V}_2\text{O}_8$	(7)
$\text{Cr}_2\text{O}_3 + 1.5\text{O}_2(\text{g}) + 2\text{CaO} \rightleftharpoons 2\text{CaCrO}_4$	(8)
$\text{Cr}_2\text{O}_3 + \text{O}_2(\text{g}) + 3\text{CaO} \rightleftharpoons \text{Ca}_3(\text{CrO}_4)_2$	(9)

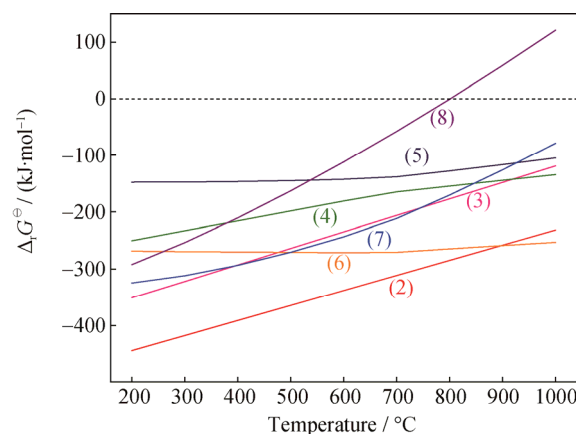


**Fig. 4. Relationship between the standard Gibbs free energy change and temperature for reactions (2)–(8).**

### 3.2. Effects of the CaO purity

As previously described, CaO can react with water in the air to form Ca(OH)<sub>2</sub>, reducing the purity of CaO. Fig. 5 shows the TG–DSC curve of the CaO used in the experiments. The endothermic peaks at 442°C and the mass loss at 549°C are in good agreement with the dehydration of bound water in CaO and the decomposition of Ca(OH)<sub>2</sub>, respectively, which lead to the actual amounts of CaO reacting with HCVS being smaller than the theoretically calculated values. To explore the effects of CaO purity, the CaO roasted at 480, 550, and 700°C for 120 min (these temperatures were selected on the basis of Fig. 5), along with the CaO without roasting were added to HCVS, and the mix-



tures were roasted at 850°C for 60 min. However, the leaching results show that the leaching ratios of vanadium and chromium under these different conditions were very similar; therefore, the purity of CaO had little effect on the vanadium and chromium extraction. These results are attributed to the fact that the reactive activity of CaO during calcification roasting is substantially higher than that of the pre-roasted CaO. This greater reactive activity can compensate for the difference between the actual reacted and the theoretically calculated CaO masses. Furthermore, the generation of gas by the decomposition of  $\text{Ca}(\text{OH})_2$  makes the solid powder porous and accelerates the gas–solid mass transfer. Hence, using the original CaO directly is convenient and efficient.

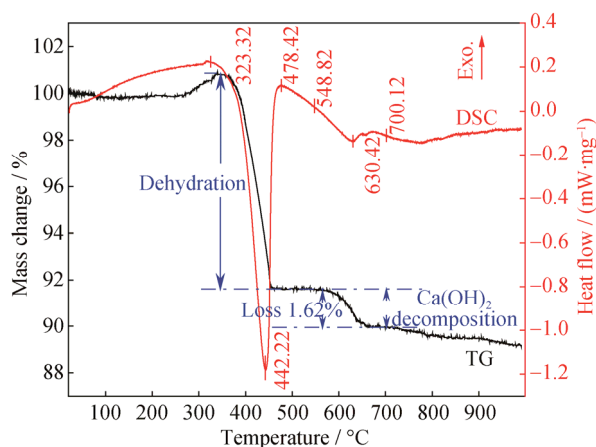


Fig. 5. TG–DSC curves of CaO.

### 3.3. Effects of the CaO amount

The addition of a calcium compound is the essential difference distinguishing calcification roasting from other roasting methods, which is why the effects of added amounts of CaO on the extraction of vanadium and chromium are discussed first. In these experiments, CaO was added to HCVS in  $n(\text{CaO})/n(\text{V}_2\text{O}_5)$  ratios from 0 to 5. The mixture was roasted at 10°C/min from room temperature to 850 or 950°C, and maintained at the target temperature for 60 min. The leaching ratios of vanadium and chromium and the concentration of total chromium with different amounts of added CaO are shown in Fig. 6. When no CaO was added, the leaching ratio of vanadium is low. When CaO was added to the HCVS gradually, the vanadium leaching ratio first increased to a maximum of 91.14% at an  $n(\text{CaO})/n(\text{V}_2\text{O}_5)$  ratio of 0.5 at 950°C and then decreased. This result demonstrates that the addition of CaO leads to a more complete oxidation of low-valence vanadium. By comparison, the variation trend of the chromium leaching ratio is opposite to that of vanadium, and the maximum leaching ratio of 8.48% is obtained at an  $n(\text{CaO})/n(\text{V}_2\text{O}_5)$  ratio of 5 with a highest

total Cr concentration of 13.73 mg/L in the leaching liquid, which indicates that the majority of chromium remains in the leaching residue. A lower Cr concentration in the liquid indicates that the vanadium waste water contains little chromium, thus avoiding a serious threat to water quality. HCVS with CaO added in an  $n(\text{CaO})/n(\text{V}_2\text{O}_5)$  ratio of 0.5 was heated at 10°C/min from room temperature to 950°C and roasted at this temperature for 60 min, the leaching ratios of vanadium and chromium reached 91.14% and 0.49%, respectively.

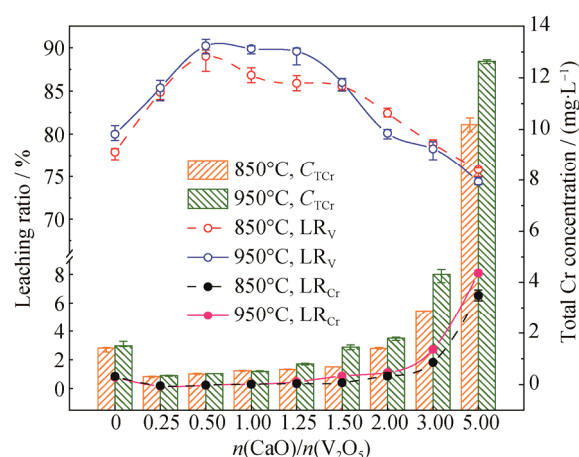
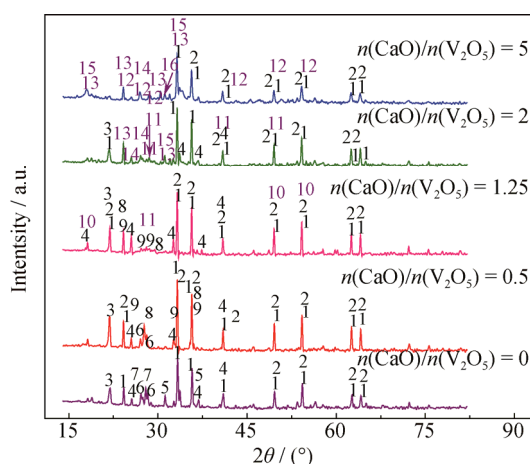


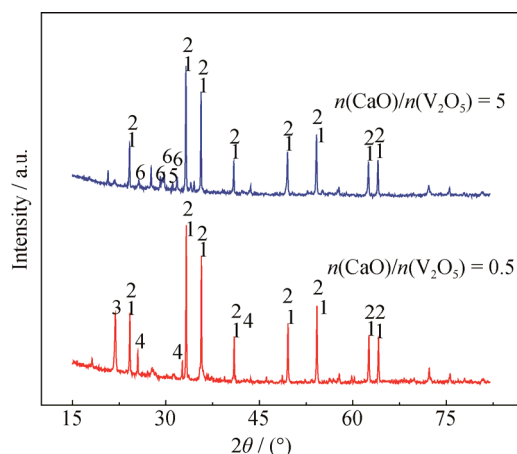
Fig. 6. Effects of the added amount of CaO on the leaching ratios of V and Cr and on the total Cr concentration (roasting temperature: 850 and 950°C; holding time: 60 min; heating rate: 10°C/min.  $C_{\text{TCr}}$  is the total Cr concentration in mg/L;  $\text{LR}_V$  and  $\text{LR}_{\text{Cr}}$  are the leaching ratios of vanadium and chromium, respectively).

Fig. 7 shows the XRD patterns of products roasted at  $n(\text{CaO})/n(\text{V}_2\text{O}_5)$  ratios from 0 to 5. For different amounts of CaO,  $\text{Fe}_2\text{O}_3$  and  $(\text{Fe}_{0.6}\text{Cr}_{0.4})_2\text{O}_3$  are the main phases with the strongest peaks, and  $\text{FeTi}_2\text{O}_5$  and  $\text{SiO}_2$  are also generated. With no addition of CaO, vanadium exists as other acid-soluble vanadates, including  $\text{Mn}_4\text{V}_2\text{O}_9$ ,  $\text{Mn}_2\text{V}_2\text{O}_7$ , and  $\text{Cr}_{0.07}\text{V}_{1.93}\text{O}_4$ . Most of the chromium forms as  $(\text{Fe}_{0.6}\text{Cr}_{0.4})_2\text{O}_3$  conjugated to Fe ions, and a small amount of chromium is incorporated into  $\text{VO}_2$  to generate  $\text{Cr}_{0.07}\text{V}_{1.93}\text{O}_4$ , which is in good agreement with previously reported results [6]. With the addition of CaO, calcium vanadates, such as  $\text{CaV}_2\text{O}_5$ ,  $\text{CaV}_2\text{O}_6$ ,  $\text{Ca}_2\text{V}_2\text{O}_7$ , and  $\text{Ca}_3\text{V}_2\text{O}_8$ , are generated gradually. Meanwhile, some chromium is oxidized and calcified as acid-soluble calcium chromates such as  $\text{CaCrO}_4$  and  $\text{Ca}_3(\text{CrO}_4)_2$ . With the addition of more CaO to HCVS, characteristic peaks of  $\text{Fe}_2\text{O}_3$ ,  $(\text{Fe}_{0.6}\text{Cr}_{0.4})_2\text{O}_3$ , and  $\text{SiO}_2$  are weakened; the peaks of  $\text{Ca}_2\text{SiO}_4$  and calcium chromate become stronger and excess calcium reacts with titanium to form calcium titanate ( $\text{Ca}_2\text{Ti}_2\text{O}_6$ ).



**Fig. 7.** XRD patterns of roasted products with the addition of different amounts of CaO to the HCVS (roasting temperature: 950°C; holding time: 60 min; heating rate: 10°C/min). 1—Fe<sub>2</sub>O<sub>3</sub>; 2—(Fe<sub>0.6</sub>Cr<sub>0.4</sub>)<sub>2</sub>O<sub>3</sub>; 3—SiO<sub>2</sub>; 4—FeTi<sub>2</sub>O<sub>5</sub>; 5—Mn<sub>4</sub>V<sub>2</sub>O<sub>9</sub>; 6—Cr<sub>0.07</sub>V<sub>1.93</sub>O<sub>4</sub>; 7—Mn<sub>2</sub>V<sub>2</sub>O<sub>7</sub>; 8—FeVO<sub>4</sub>; 9—CaV<sub>2</sub>O<sub>5</sub>; 10—CaV<sub>2</sub>O<sub>6</sub>; 11—Ca<sub>2</sub>V<sub>2</sub>O<sub>7</sub>; 12—Ca<sub>3</sub>V<sub>2</sub>O<sub>8</sub>; 13—CaCrO<sub>4</sub>; 14—Ca<sub>3</sub>(CrO<sub>4</sub>)<sub>2</sub>; 15—Ca<sub>2</sub>SiO<sub>4</sub>; 16—Ca<sub>2</sub>Ti<sub>2</sub>O<sub>6</sub>.

The XRD patterns of the leaching residues are shown in Fig. 8. A comparison of the phases before and after leaching indicates that, for an  $n(\text{CaO})/n(\text{V}_2\text{O}_5)$  ratio of 0.5, vanadates such as Cr<sub>0.07</sub>V<sub>1.93</sub>O<sub>4</sub>, FeVO<sub>4</sub>, and CaV<sub>2</sub>O<sub>5</sub>, whose peaks are concentrated in the range from 27 to 32°, vanished after leaching, whereas Fe<sub>2</sub>O<sub>3</sub> or (Fe<sub>0.6</sub>Cr<sub>0.4</sub>)<sub>2</sub>O<sub>3</sub> and SiO<sub>2</sub> remain in the leaching residue, thus achieving efficient extraction of vanadium from HCVS. For an  $n(\text{CaO})/n(\text{V}_2\text{O}_5)$  ratio of 5, vanadates and chromates such as Ca<sub>3</sub>V<sub>2</sub>O<sub>8</sub>, CaCrO<sub>4</sub>, and Ca<sub>3</sub>(CrO<sub>4</sub>)<sub>2</sub> dissolve, whereas Ca<sub>2</sub>Ti<sub>2</sub>O<sub>6</sub> remains in the solid residue; in addition, calcium combines with sulfate in the leaching medium and forms acid-insoluble calcium sulfate.



**Fig. 8.** XRD patterns of leaching residues from samples with different amounts of CaO addition (roasting temperature: 950°C; holding time: 60 min; heating rate: 10°C/min). 1—Fe<sub>2</sub>O<sub>3</sub>; 2—(Fe<sub>0.6</sub>Cr<sub>0.4</sub>)<sub>2</sub>O<sub>3</sub>; 3—SiO<sub>2</sub>; 4—FeTi<sub>2</sub>O<sub>5</sub>; 5—Ca<sub>2</sub>Ti<sub>2</sub>O<sub>6</sub>; 6—CaSO<sub>4</sub>·0.5H<sub>2</sub>O.

In addition, the color of the leaching liquid clearly changed as the amount of CaO added and the roasting temperature of the HCVS were varied, as shown in Fig. 9. The leaching liquid corresponding to the sample roasted at 850°C is blue-green, whereas the sample roasted at 950°C is yellow and becomes darker with increasing amounts of CaO. In acidic solution, V(IV) exists in the form of blue VO<sub>2</sub><sup>+</sup>, V(V) is yellow in the form of VO<sub>2</sub><sup>+</sup>, Cr(III) is green, and Cr(VI) is orange. The color change implies that, at lower temperatures, the oxidation of low-valence vanadium is incomplete and most of the vanadium ions are in a tetravalent or a nonstoichiometric valence state. Further, with increasing roasting temperature, the leaching liquid becomes yellow because of the formation of a higher-valence vanadate. The XRD patterns of the leaching residue, shown in Fig. 8, also demonstrate that the yellow color of the leaching liquid was not caused by Fe<sup>3+</sup> ions.

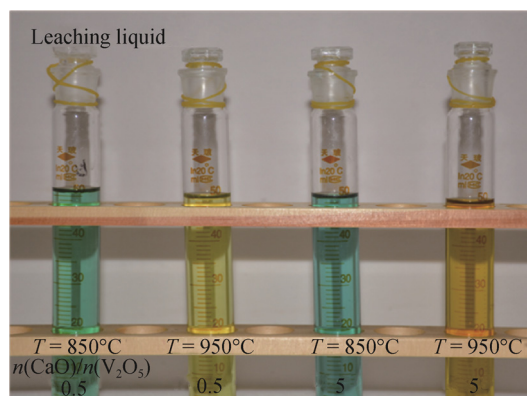


**Fig. 9.** Images of the leaching liquids.

Notably, the leaching ratio of vanadium at an  $n(\text{CaO})/n(\text{V}_2\text{O}_5)$  ratio of 0.5 is only slightly higher than that with an  $n(\text{CaO})/n(\text{V}_2\text{O}_5)$  ratio of 1.25 at 950°C, as shown in Fig. 6. Further, the addition of more CaO is beneficial for studying the interaction of CaO with vanadium and chromium. With the addition of more CaO, clear peaks of calcium chromate appear, as displayed in Fig. 7. Furthermore, in practical experiments, we found that CaO can avoid material sintering to a certain extent, and with the addition of more CaO, the roasted samples become looser, which is convenient for subsequent grinding and leaching. Hence, we chose an  $n(\text{CaO})/n(\text{V}_2\text{O}_5)$  ratio of 1.25 as the condition for the CaO amount in the experiments discussed in sections 3.4, 3.5, and 3.6.

### 3.4. Effects of roasting temperature

Roasting temperature is a key parameter for calcification roasting, and the effects of this parameter were investigated

from 600 to 950°C (Fig. 10). In this experiment, CaO was added to HCVS in an  $n(\text{CaO})/n(\text{V}_2\text{O}_5)$  ratio of 1.25. The mixture was heated at 10°C/min from room temperature and maintained at the target temperature for 60 min. With increasing temperature, the leaching ratio of vanadium increases continuously and reaches a maximum of 90.63% at 950°C, indicating that the oxidation and calcification of vanadium proceeds until a certain reaction temperature is reached. The experiment demonstrates that roasting at higher temperatures does not lead to material sintering, which can be attributed to the process of heating by temperature programming, furnace cooling, and a shorter roasting time. This phenomena differs from those reported in other studies [22]. For the oxidation of chromium, as the temperature rises from 600 to 900°C, the leaching ratio decreases from 4.45% to 0.28%. The highest total Cr concentration at 600°C is less than 10 mg/L. With a further increase in temperature to 950°C, the leaching ratio increases to 0.80%. The variation trend of the total Cr concentration is consistent with that of the chromium leaching ratio.

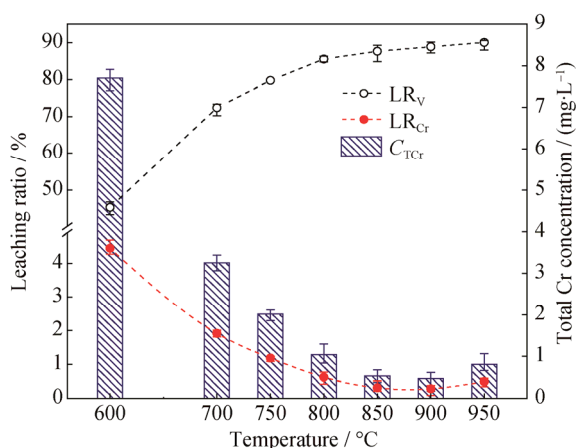


**Fig. 10.** Effects of roasting temperature on the leaching ratios of V and Cr and on the total Cr concentration ( $n(\text{CaO})/n(\text{V}_2\text{O}_5) = 1.25$ ; holding time: 60 min; heating rate: 10°C/min).

Fig. 11 shows the phase composition of products roasted at different temperatures. A series of  $\text{Fe}_2\text{O}_3$  and  $(\text{Fe}_{0.6}\text{Cr}_{0.4})_2\text{O}_3$  peaks are observed, and these are the main phase. At 600°C, the olivine phase  $(\text{Fe,Mn})_2\text{SiO}_4$  disappears and  $\text{SiO}_2$  is found, suggesting that oxidation and decomposition of the olivine phase occur before 600°C. Some acid-soluble vanadates, such as  $\text{Cr}_{0.07}\text{V}_{1.93}\text{O}_4$  and  $\text{Mn}_4\text{V}_2\text{O}_9$ , are also generated at 600°C, and most of the chromium also exists in the form of  $(\text{Fe}_{0.6}\text{Cr}_{0.4})_2\text{O}_3$ . At 700°C, the peaks of  $\text{Fe}_2\text{O}_3$ ,  $(\text{Fe}_{0.6}\text{Cr}_{0.4})_2\text{O}_3$ , and  $\text{SiO}_2$  are stronger, con-

sistent with the further decomposition and oxidation of spinels. At 850°C, calcium vanadates appear gradually, leading to an increase in the vanadium leaching ratio. Meanwhile, no calcium chromate peak is detected, indicating that very little chromium has reacted with CaO. At 950°C, the intensity of almost all of the peaks increases, implying that oxidation and calcification are comparatively complete.

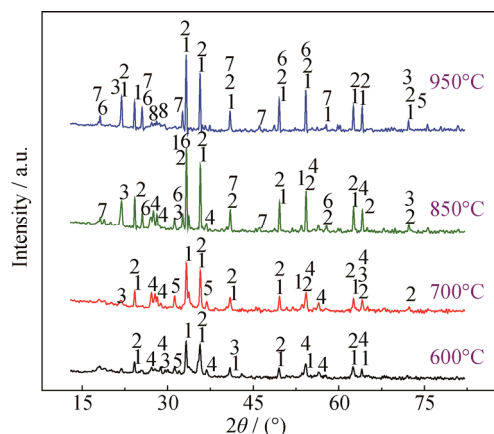


**Fig. 11.** XRD patterns of products roasted at 600, 700, 850, and 950°C ( $n(\text{CaO})/n(\text{V}_2\text{O}_5) = 1.25$ ; holding time: 60 min; heating rate: 10°C/min). 1— $\text{Fe}_2\text{O}_3$ ; 2— $(\text{Fe}_{0.6}\text{Cr}_{0.4})_2\text{O}_3$ ; 3— $\text{SiO}_2$ ; 4— $\text{Cr}_{0.07}\text{V}_{1.93}\text{O}_4$ ; 5— $\text{Mn}_4\text{V}_2\text{O}_9$ ; 6— $\text{CaV}_2\text{O}_6$ ; 7— $\text{FeTi}_2\text{O}_5$ ; 8— $\text{CaV}_2\text{O}_5$ .

### 3.5. Effects of holding time

To optimize the holding time of calcification roasting, CaO was added to HCVS in an  $n(\text{CaO})/n(\text{V}_2\text{O}_5)$  ratio of 1.25 and the mixture was heated at 10°C/min from room temperature to 850°C and maintained at this temperature for 0–180 min. The leaching ratios of vanadium and chromium and the total chromium concentration at different holding times are shown in Fig. 12. The results show that, with increasing holding time, the leaching ratio of vanadium gradually increases, reaching a maximum of 91.02% at 180 min. Further, the variation trend of the chromium leaching ratio is opposite to that of vanadium, which reaches a maximum of 0.79% at 0 min and decreases continuously with time. The highest total Cr concentration is only 1.33 mg/L. Prolonging the reaction time can promote oxidation and calcification of spinels. The leaching ratios of vanadium and chromium exhibit opposite trends because of the competitive relationship between vanadium and chromium. By comprehensively considering the cost of the process, along with the leaching ratios of vanadium and chromium, we found that roasting HCVS for 60 min is feasible.

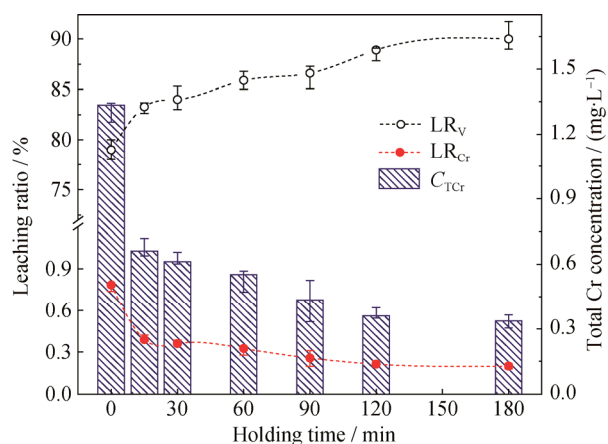


Fig. 12. Effects of holding time on the leaching ratios of V and Cr and on the total Cr concentration ( $n(\text{CaO})/n(\text{V}_2\text{O}_5) = 1.25$ ; roasting temperature:  $850^\circ\text{C}$ ; heating rate:  $10^\circ\text{C}/\text{min}$ ).

### 3.6. Effects of heating rate

As reported previously [22], the leaching of vanadium during calcification roasting is strongly affected by the heating rate. Besides, the different heating rates should be carried out to elucidate further the factors that influence the chromium extraction. HCVS mixed in an  $n(\text{CaO})/n(\text{V}_2\text{O}_5)$  ratio of 1.25 was heated from room temperature to  $850^\circ\text{C}$  at heating rates of 2, 5, 10, 15, and  $30^\circ\text{C}/\text{min}$  by adjusting the temperature controller of the muffle furnace; the samples were then maintained at  $850^\circ\text{C}$  for 60 min. The leaching ratios of vanadium and chromium are shown in Fig. 13. The maximum vanadium leaching ratio is 87.35% at  $2^\circ\text{C}/\text{min}$ . When the heating rate was increased from 2 to  $30^\circ\text{C}/\text{min}$ , the leaching ratio of vanadium gradually decreased. As previously described, the spinel phase is wrapped by the olivine phase, implying that the more thorough the decomposition of the olivine phase, the more the spinel phase is exposed with a larger contact area and the more completely the spinel phase is oxidized and calcified. The leaching ratio of chromium was expected to exhibit the opposite trend as that of vanadium and to gradually decrease with increasing heating rate because of the competitive reaction. In the experiment, the leaching ratio of chromium first decreased and then increased, reaching a minimum of 0.18% at a heating rate of  $10^\circ\text{C}/\text{min}$ . This trend is attributed to that calcification roasting of HCVS is comparatively driven to completion at the lower heating rates of 2 and  $5^\circ\text{C}/\text{min}$ , weakening the reactive competition between vanadium and chromium with CaO. Further, the highest Cr concentration is lower than 1 mg/L.

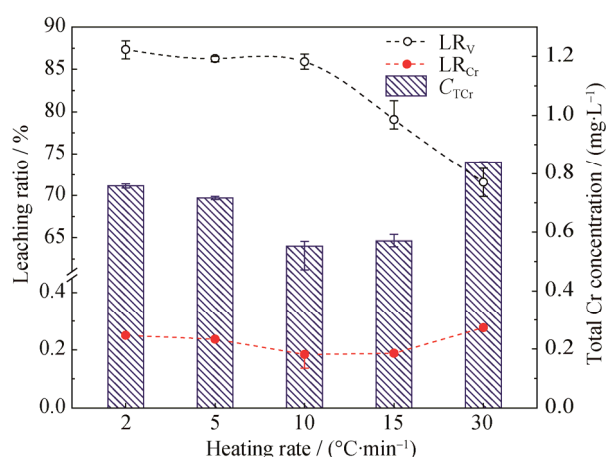
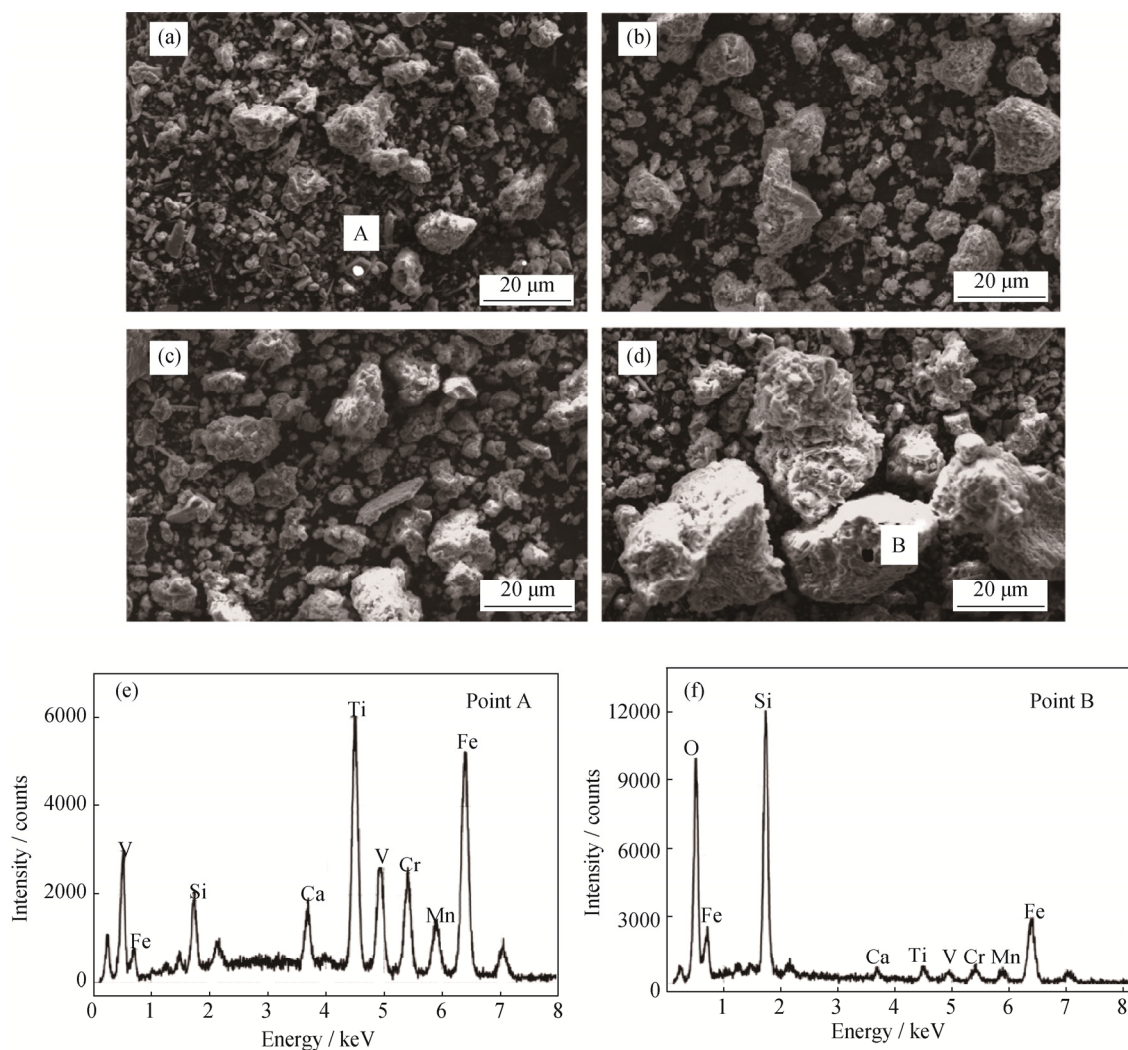


Fig. 13. Effects of heating rate on the leaching ratios of V and Cr and on the total Cr concentration ( $n(\text{CaO})/n(\text{V}_2\text{O}_5) = 1.25$ ; roasting temperature:  $850^\circ\text{C}$ ; holding time: 60 min).

Fig. 14 shows the SEM micrographs of the products roasted at different heating rates. Three samples were roasted at 2, 10, and  $30^\circ\text{C}/\text{min}$  using temperature programming by adjusting the parameters of the muffle furnace. The fourth sample was placed in the muffle furnace when the furnace temperature reached  $850^\circ\text{C}$ . This fourth sample did not experience the heating program, and the heating rate and heating time were not detected and measured because the heating was instantaneous. The diameters of the crystal grains in the product roasted at  $2^\circ\text{C}/\text{min}$  in Fig. 14(a) are relatively small, and the surface of the grains is smooth and light. With increasing heating rate, an increasing number of tiny, light, irregular particles are wrapped, and the crystal grain size gradually increases, as shown in Figs. 14(b) and 14(c). Furthermore, the package phenomenon is serious for the roasted product that did not experience the temperature programming of the furnace in Figs. 14(d). According to further research by EDS analysis, region A in Fig. 14(a) consists of vanadium, chromium, and titanium, indicating that the tiny, light particles may be the oxidation and calcification products of vanadium or chromium. However, the EDS analysis of point B shows that silicon, iron, and oxygen are the main elements in Fig. 14(d), demonstrating that the wrapped particles may be the olivine phase failing to decompose thoroughly or the components with low melting points. All of these scenarios indicate that roasting samples at a higher heating rate is unfavorable for the complete decomposition of olivine, hindering the further oxidation of spinels and causing a decrease in the vanadium leaching ratio. Given the cost and efficiency of production, a heating rate of  $10^\circ\text{C}/\text{min}$  is the most suitable heating rate for production.





**Fig. 14.** SEM micrographs of products roasted at 850°C with different heating rates: (a) 2°C/min, (b) 10°C/min, and (c) 30°C/min; (d) the product not subjected to the temperature program of the furnace and placed in a muffle furnace preheated to 850°C; (e, f) EDS analyses of points A in (a) and B in (d).  $n(\text{CaO})/n(\text{V}_2\text{O}_5) = 1.25$ ; roasting temperature: 850°C; holding time: 60 min.

Notably, when the HCVS with CaO added in an  $n(\text{CaO})/n(\text{V}_2\text{O}_5)$  ratio of 0.5 was roasted in an air atmosphere at a heating rate of 10°C/min from room temperature to 950°C and maintained at this temperature for 60 min, the vanadium leaching ratio reached a maximum, and almost all of the chromium remained in the leaching residue. Thus, the results not only indicate that the vanadium was efficiently extracted from the HCVS, but also suggest a possible new approach to separate vanadium and chromium. Table 3 shows the typical composition of the leaching liquid. The concentration of vanadium is much greater than that of the other components, indicating that vanadium can be extracted efficiently from HCVS by calcification roasting–acid leaching. Further, chromium is not leached and translated into the leaching solution, thereby enabling the efficient ex-

traction of vanadium and creating favorable conditions for chromium extraction in the next step. The concentration of silicon, which is harmful to the final product  $\text{V}_2\text{O}_5$ , is lower and does not affect the product quality.

**Table 3.** Concentrations of the main components in the leaching liquid

g/L					
V	Cr	Ti	Fe	Si	Mn
0.24	0.001	$1.5 \times 10^{-3}$	0.013	0.002	0.065

### 3.7. Analysis of oxidation and calcification processes

On the basis of the aforementioned experiments and analyses, the interaction of CaO with vanadium and chromium in HCVS during calcification roasting was characterized; a schematic of the process is shown in Fig. 15, where spheres

of various colors represent different substances whose amounts represent only the relative content. With the gradual addition of CaO, calcium vanadates and calcium chromate are generated gradually until CaO remains.

The maximum leaching ratio of vanadium of 91.14% and the maximum leaching ratio of chromium of 8.48% are

achieved at  $n(\text{CaO})/n(\text{V}_2\text{O}_5)$  ratios of 0.5 and 5, respectively. We therefore studied the oxidation and calcification processes of these two cases with HCVS using dynamic heating experiments (TG–DSC). Figs. 16(a) and 16(b) show

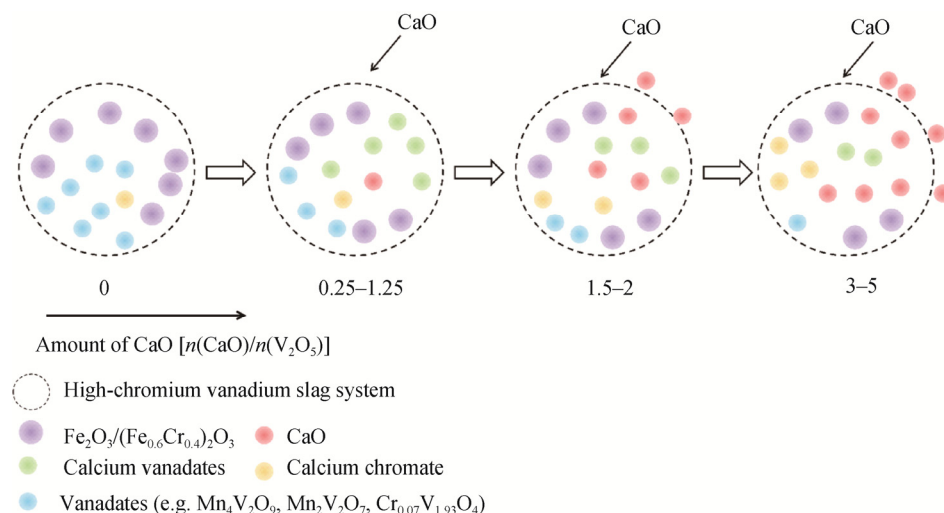


Fig. 15. Schematic of the process of calcification roasting.

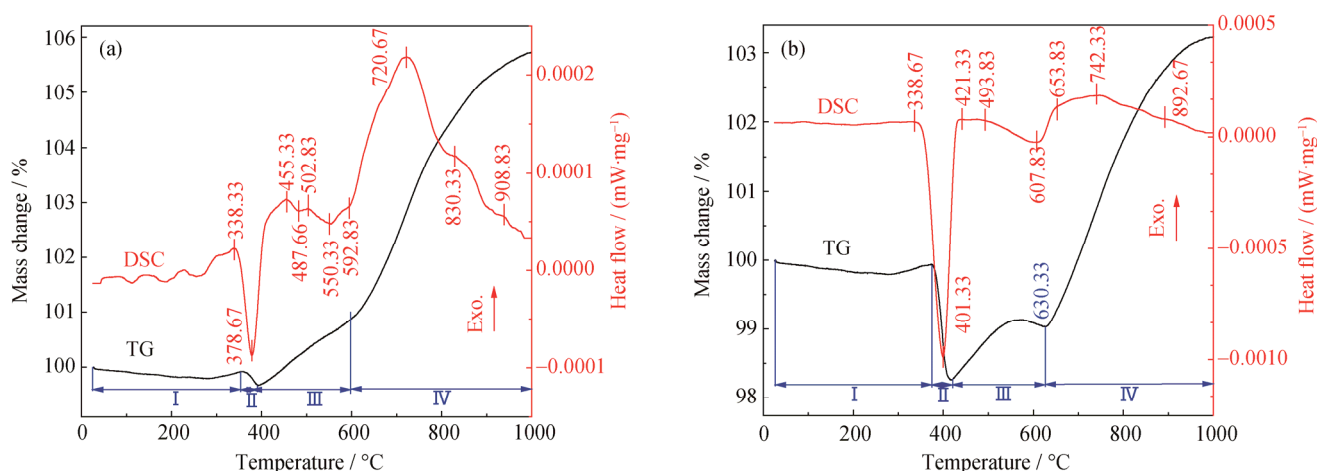


Fig. 16. TG–DSC curves of HCVS with CaO at an  $n(\text{CaO})/n(\text{V}_2\text{O}_5)$  ratio of 0.5 (a) and 5 (b).

TG–DSC curves corresponding to  $n(\text{CaO})/n(\text{V}_2\text{O}_5)$  ratios of 0.5 and 5, respectively, heated at  $10^\circ\text{C}/\text{min}$  from room temperature to  $1000^\circ\text{C}$ . In the DSC thermogram, the exothermic peaks are in agreement with the oxidation and calcification processes of free iron, olivine, and spinels, and the endothermic peaks are in agreement with the dehydration and decomposition of  $\text{Ca}(\text{OH})_2$ , olivine, and spinels. From the thermogram corresponding to the  $n(\text{CaO})/n(\text{V}_2\text{O}_5)$  ratio of 0.5 (Fig. 16(a)), four stages are observed during the reaction process. During stage I (room temperature to  $340^\circ\text{C}$ ), the decrease in sample mass and several endothermic peaks indicate the vola-

tilization of free water in HCVS and CaO in the first half, and the small increase in the mass in the second half indicates the partial oxidation. At stage II ( $340\text{--}390^\circ\text{C}$ ), the remarkable mass loss is consistent with the removal of bound water in CaO and HCVS. At stage III ( $390\text{--}592^\circ\text{C}$ ), the sample mass increases by approximately 1.0% and some exothermic peaks appear. According to the XRD analysis discussed in section 3.4, the olivine phase decomposed before  $600^\circ\text{C}$ , indicating that the oxidation of olivine occurs at stage III. Further, the endothermic peak at  $550^\circ\text{C}$  is in good agreement with the  $\text{Ca}(\text{OH})_2$  decomposition. At stage IV ( $592\text{--}1000^\circ\text{C}$ ), the

weight of the sample increased by 4.88%, and some exothermic peaks exist at 721, 830, and 909°C. Combining with the XRD analyses presented in sections 3.3 and 3.4, spinels is oxidized and calcified at this stage.

For the sample with an  $n(\text{CaO})/n(\text{V}_2\text{O}_5)$  ratio of 5 (Fig. 16(b)), the reaction process is similar to that with an  $n(\text{CaO})/n(\text{V}_2\text{O}_5)$  ratio of 0.5; however, the final temperatures for stage II and III shift to higher temperatures of 420°C and 630°C, respectively, possibly because of the different amounts of CaO. Furthermore, a stronger endothermic peak appears at 401°C, which corresponds to the dehydration of increased amounts of CaO, and accompanies an obvious mass loss due to increased  $\text{Ca}(\text{OH})_2$  decomposition, consistent with the TG–DSC curve of CaO in Fig. 5. The oxidation and calcification of vanadium and chromium in spinels occurs at 592°C and 630°C for  $n(\text{CaO})/n(\text{V}_2\text{O}_5)$  ratios of 0.5 and 5, respectively. Notably, the oxidation and calcification temperatures of the spinels differ from those previously reported [22], which is attributed to the difference in heating rates and to the higher content of  $\text{Cr}_2\text{O}_3$  in the vanadium slag.

#### 4. Evaluation

The separation of vanadium and chromium is an important and difficult aspect for the development and utilization of vanadium–titanium-bearing magnetite. In recent years, numerous methods have been proposed to solve this problem. In particular, Li *et al.* [8] proposed the asynchronous extraction of vanadium and chromium from vanadium slag by stepwise sodium roasting–water leaching based on the nucleation and growth kinetics of spinel crystals in vanadium slag. This provided a novel method by which to separate vanadium and chromium by controlling the roasting conditions rather than by separating them in the liquid phase. By contrast, Li *et al.* [7] and Wang *et al.* [11] reported that chromium is more likely to combine with sodium salt and form soluble sodium chromate during sodium salt roasting–water leaching; their different results suggest that the extraction of chromium during sodium roasting relies heavily on the raw materials and the roasting parameters. Meanwhile, the inherent defects of sodium roasting, such as material sintering, the generation of harmful gases, and the potential environmental threat from the remaining soluble vanadium and chromium in the tailings, restricted the development of sodium roasting.

For the calcification roasting demonstrated in this work, under the experimental conditions the vanadium leaching ratio is greater than 90%, and almost no chromium is ex-

tracted in the leaching liquid; more vanadium and less chromium are extracted compared with previously reported methods. Furthermore, calcification roasting can prevent sintering and the generation of harmful gases and the remaining vanadium and chromium in the tailings are insoluble, avoiding the threat to water. Hence, extracting vanadium and chromium step by step by calcification roasting may be a new environmentally friendly method to separate vanadium and chromium, which is meaningful as a subject of study in future research.

#### 5. Conclusions

In this study, the extraction behavior of vanadium and chromium during calcification roasting of HCVS was investigated systematically. The conclusions are summarized as follows:

(1) Increasing the roasting temperature, lowering the heating rate to an appropriate rate, and prolonging the holding time are beneficial to vanadium oxidation. Relatively high vanadium and low chromium leaching ratios of 91.14% and 0.49%, respectively, were achieved under the optimal roasting conditions of an  $n(\text{CaO})/n(\text{V}_2\text{O}_5)$  ratio of 0.5, a roasting temperature of 950°C, a heating rate of 10°C/min, and a holding time of 60 min.

(2) Phase composition analyses indicated that, with the addition of CaO, most of the vanadium reacted to form acid-soluble calcium vanadates such as  $\text{CaV}_2\text{O}_6$ ,  $\text{Ca}_2\text{V}_2\text{O}_7$ , and  $\text{Ca}_3\text{V}_2\text{O}_8$ . In addition, almost all of the chromium in the form of  $(\text{Fe}_{0.6}\text{Cr}_{0.4})_2\text{O}_3$  remained in the leaching residue; only a small amount of chromium reacted with CaO to form acid-soluble chromates. This research thus provides a new method for separating vanadium and chromium.

(3) A competitive reaction occurs when vanadium and chromium react with CaO, and vanadium tends to react with CaO to generate vanadates. Consequently, opposite variation trends were observed in the vanadium and chromium leaching ratios, consistent with the thermodynamic analysis.

(4) The entire calcification roasting reaction included the following steps: dehydration of free and bound water in HCVS and CaO, oxidation of free iron, decomposition and oxidation of olivine, and oxidation and calcification of spinels. The oxidation and calcification of spinels occurred at 592°C and 630°C for  $n(\text{CaO})/n(\text{V}_2\text{O}_5)$  ratios of 0.5 and 5, respectively; this difference was attributed to the different amounts of added CaO.

#### Acknowledgements

This research was financially supported by the National Natural Science Foundation of China (Nos. 51604065 and 51574082), the National Basic Research Program of China (No. 2013CB632603), and the Fundamental Funds for the Central Universities (Nos. 150203003 and 150202001).

## References

- [1] R.R. Moskalyk and A.M. Alfantazi, Processing of vanadium: a review, *Miner. Eng.*, 16(2003), No. 9, p. 793.
- [2] B. Dhal, H.N. Thatoi, N.N. Das, and B.D. Pandey, Chemical and microbial remediation of hexavalent chromium from contaminated soil and mining/metallurgical solid waste: a review, *J. Hazard. Mater.*, 250-251(2013), p. 272.
- [3] B. Liu, H. Du, N.S. Wang, Y. Zhang, S.L. Zheng, L.J. Li, and D.H. Chen, A novel method to extract vanadium and chromium from vanadium slag using molten NaOH–NaNO<sub>3</sub> binary system, *AIChE J.*, 59(2013), No. 2, p. 541.
- [4] X.S. Li, B. Xie, G.E. Wang, and X.J. Li, Oxidation process of low-grade vanadium slag in presence of Na<sub>2</sub>CO<sub>3</sub>, *Trans. Nonferrous Met. Soc. China*, 21(2011), No. 8, p. 1860.
- [5] S.A. Katz and H. Salem, The toxicology of chromium with respect to its chemical speciation: a review, *J. Appl. Toxicol.*, 13(1993), No. 3, p. 217.
- [6] X.F. Zhang, F.G. Liu, X.X. Xue, and T. Jiang, Effects of microwave and conventional blank roasting on oxidation behavior, microstructure and surface morphology of vanadium slag with high chromium content, *J. Alloys Compd.*, 686(2016), p. 356.
- [7] M. Li, L. Xiao, J.J. Liu, Z.X. Shi, Z.B. Fu, Y. Peng, P.Z. Long, and Y.J. Yang, Effective extraction of vanadium and chromium from high chromium content vanadium slag by sodium roasting and water leaching, *Mater. Sci. Forum*, 863(2016), p. 144.
- [8] H.Y. Li, H.X. Fang, K. Wang, W. Zhou, Z. Yang, X.M. Yan, W.S. Ge, Q.W. Li, and B. Xie, Asynchronous extraction of vanadium and chromium from vanadium slag by stepwise sodium roasting-water leaching, *Hydrometallurgy*, 156(2015), p. 124.
- [9] C.P.J. Van Vuuren and P.P. Stander, The oxidation of FeV<sub>2</sub>O<sub>4</sub> by oxygen in a sodium carbonate mixture, *Miner. Eng.*, 14(2001), No. 7, p. 803.
- [10] Z.H. Wang, S.L. Zheng, S.N. Wang, B. Liu, D.W. Wang, H. Du, and Y. Zhang, Research and prospect on extraction of vanadium from vanadium slag by liquid oxidation technologies, *Trans. Nonferrous Met. Soc. China*, 24(2014), No. 5, p. 1273.
- [11] H.G. Wang, M.Y. Wang, and X.W. Wang, Leaching behaviour of chromium during vanadium extraction from vanadium slag, *Miner. Process. Extr. Metall. Rev.*, 124(2015), No. 3, p. 127.
- [12] T. Ölmez, The optimization of Cr(VI) reduction and removal by electrocoagulation using response surface methodology, *J. Hazard. Mater.*, 162(2009), No. 2-3, p. 1371.
- [13] B. Robert and F. Harry, Separation of chromium from vanadium by extraction of perchromic acid with ethyl acetate, *Anal. Chem.*, 23(1951), No. 8, p. 1110.
- [14] Y.Y. Fan, X.W. Wang, and M.Y. Wang, Separation and recovery of chromium and vanadium from vanadium-containing chromate solution by ion exchange, *Hydrometallurgy*, 136(2013), p. 31.
- [15] P. Cao, Research on vanadium slag roasted with calcium salt, *Iron Steel Vanadium Titanium*, 33(2012), No. 1, p. 30.
- [16] B.V. Slobodin, V.A. Zhilaev, A.A. Fotiev, I.A. Arapova, and N.P. Tugova, A thermoanalytical study of the interaction of vanadium(V) with calcium oxide and calcium carbonate, *J. Therm. Anal.*, 15(1979), No. 2, p. 197.
- [17] J.H. Zhang, W. Zhang, and Z.L. Xue, Oxidation kinetics of vanadium slag roasting in the presence of calcium oxide, *Miner. Process. Extr. Metall. Rev.*, 38(2017), No. 5, p. 1.
- [18] X. Zhang, B. Xie, J. Diao, and X.J. Li, Nucleation and growth kinetics of spinel crystals in vanadium slag, *Ironmaking Steelmaking*, 39(2013), No. 2, p. 147.
- [19] J. Diao, Y. Qiao, X. Zhang, C.Q. Ji, and B. Xie, Growth mechanisms of spinel crystals in vanadium slag under different heat treatment conditions, *CrystEngComm*, 17(2015), No. 38, p. 7300.
- [20] P. Miretzky and A.F. Cirelli, Cr(VI) and Cr(III) removal from aqueous solution by raw and modified lignocellulosic materials: A review, *J. Hazard. Mater.*, 180(2010), No. 1-3, p. 1.
- [21] H.Y. Hu, Z. Xu, H. Liu, D.K. Chen, A.J. Li, H. Yao, and I. Naruse, Mechanism of chromium oxidation by alkali and alkaline earth metals during municipal solid waste incineration, *Proc. Combust. Inst.*, 35(2015), No. 2, p. 2397.
- [22] J.H. Zhang, W. Zhang, L. Zhang, and S.Q. Gu, Mechanism of vanadium slag roasting with calcium oxide, *Int. J. Miner. Process.*, 138(2015), p. 20.